1   **Title: Fine-scale animal proximity detection and localization via multi-sensor biologgers**

2

3   **Author List:**

4   Will Rogers[1], Sierra J Mattingly[2,3], Jenna E Kohles[2,3,4,5], Nils Linek[2], Hannah J Williams[2,3,4],

5   Ivan Lenzi[2], Georg Wilbs[2], Marcel Escher[2], Nina Richter[2], Louis van Schalkwyk[2,6,7], Vanessa O

6   Ezenwa[1], Martin Wikelski[2,3], Dina KN Dechmann[2,3], Timm A Wild[2]

7

8   **Affiliations:**

9   [1]Department of Ecology and Evolutionary Biology, Yale University, New Haven, CT, USA

10   [2]Department of Migration, Max Planck Institute of Animal Behavior, Radolfzell, Germany

11   [3]Department of Biology, University of Konstanz, Konstanz, Germany

12   [4]Centre for the Advanced Study of Collective Behaviour, University of Konstanz, Konstanz,

13   Germany

14   [5]Smithsonian Tropical Research Institute, Panama, Republic of Panama

15   [6]Office of the State Veterinarian, Department of Agriculture, Land Reform and Rural

16   Development, Kruger National Park, Skukuza, South Africa

17   [7]Department of Veterinary Tropical Diseases, Faculty of Veterinary Science, University of

18   Pretoria, Pretoria, South Africa

19

20   **Corresponding Author:**

21   Will Rogers

22   Department of Ecology and Evolutionary Biology, 165 Prospect Street, Yale University, New

23   Haven, CT, USA 06511

24 will.rogers@yale.edu, rogerswill47@gmail.com

25

26 **Running Headline:** Proximity and localization using biologgers

27

30

41

47   data was collected, and data collection was performed with involvement and approval from

48   relevant authorities.

49

50   **Data Availability:** A zip file containing data, code necessary to reproduce the results in the

51   paper, and compiled code is at the time of submission. Data will be stored with Zenodo upon

52   acceptance.

53   **Conflicts of Interest**: We have no conflicts of interest to disclose.

54   **Abstract:**

55   1.   Accurately quantifying spatial interactions is central to understanding social behavior,

56   information flow, predator-prey dynamics, and disease transmission. Proximity loggers

57   that record received signal strength indicator (RSSI) offer a promising approach for

58   estimating pairwise distances, particularly in environments where GPS is unavailable or

59   imprecise. However, RSSI is often dismissed as too noisy for fine-scale inference, with

60   performance that depends on environmental conditions, tag orientation, and between-

61   device variability. Incorporating additional tag-measured data may improve RSSI

62   performance and enable its use as a continuous measure of distance in variable

63   environments.

64   2.   Here, we assess the utility of continuous RSSI as a fine-scale distance estimator and

65   localization tool using a novel multi-sensor WiFi biologger (WildFi). We conducted four

66   experiments: (1) testing how tag orientation affects RSSI-distance relationships; (2)

67   evaluating whether environmental covariates measured by onboard sensors improve

68   proximity estimates; (3) assessing the accuracy of trilateration-based tag localization

69   using fixed gateway arrays; and (4) comparing RSSI- and GPS-inferred proximity in free-

70   ranging Egyptian fruit bats (*Rousettus aegyptiacus*).

71   3.   While RSSI alone could predict distance with reasonable accuracy, incorporating

72   additional tag-sensed information (*e.g.*, temperature, humidity, barometric pressure) and

73   accounting for tag-level heterogeneity significantly improved predictive accuracy. Based

74   on RSSI predictions, we could estimate tag location with a median error of 2.6 meters,

75   accurate enough to indirectly estimate proximity networks without tag-to-tag

76   communication. In deployments on free-flying bats, we found that RSSI and GPS were

77   only weakly concordant, with GPS unreliable for detecting fine-scale interactions (<50

78   m). In contrast, RSSI could capture both fine-scale and some long-range interactions up

79   to ~250m.

80   4. These findings highlight RSSI's potential as a robust metric for proximity logging,

81   particularly when combined with multi-sensor data and pre-deployment validations.

82   Integrating multi-sensor data streams further enhances RSSI interpretability. Future

83   biologger designs should prioritize synergy among data streams for integrated insights

84   into proximity and animal behavior.

85

86   **Data and code for peer review statement:** Data and code to reproduce the results of the paper

87   are provided in a zip folder for peer review. We also provided our compiled code.

88

89   **Keywords:** Proximity logging, biologging, received signal strength indicator (RSSI),

90   trilateration, sensor validation, animal interactions, social behavior

91

92   **Introduction:**

93   Measuring fine-scale interactions between animals is essential for understanding social

94   structure, information exchange, predator-prey dynamics, and disease transmission (Krause et al.

95   2013, Smith and Pinter-Wollman 2021, Suraci et al. 2022), processes with implications for

96   conservation and management (Snijders et al. 2017). These processes depend not only on

97   whether animals encounter each other, but also how close they are, how often they interact, and

98   for how long—requiring tools that capture proximity at relevant spatial and temporal scales.

99   Wireless technologies like Bluetooth Low Energy (BLE) and WiFi offer one such solution by

100   recording received signal strength indicator (RSSI), which declines with distance and can serve

101   as a continuous proxy for proximity between animal-borne sensors. While many RSSI

102   applications discretize interactions into binary "contact" or "non-contact" events (Cross et al.

103   2012), these thresholds can be misaligned with underlying biological processes and obscure

104   important variation in interaction frequency, duration, or intensity (Craft 2015). Treating RSSI as

105   a continuous variable rather than a discrete contact metric may provide more nuanced and

106   biologically interpretable insights into proximity-dependent processes without imposing rigid

107   assumptions about contact definitions (St Clair et al. 2015, Ripperger et al. 2016).

108   However, RSSI-based distance estimates are sensitive to environmental and technical

109   variation (Drewe et al. 2012, Bettaney et al. 2015, Rutz et al. 2015), such as ambient weather

110   conditions (Marfievici et al. 2013), the habitat structure (Böhm et al. 2009), antenna orientation

111   (Prange et al. 2006), and variation between tags (Boyland et al. 2013). These sources of variation

112   may reduce the precision of RSSI-based estimates, particularly in field conditions. This leaves

113   open questions about whether RSSI can serve as an accurate proxy of distance and how to refine

114   RSSI predictions.

115   One approach to enhance RSSI performance is to combine them with other tag-sensed

116   information related to RSSI signal error. For example, multi-sensor biologgers are devices that

117   integrate multiple sensing modalities on the same tag, supporting inferences beyond single

118   sensors alone (Williams et al. 2020). Because RSSI is influenced by weather, collecting

119   temperature, humidity, or barometric pressure simultaneously with RSSI could offer pathways to

120   account for these sources of variation, estimating distance as a function of multiple data streams

121   beyond RSSI alone. Multi-sensor approaches remain largely untested in proximity logging –

122   especially in free-ranging animals and under real-world environmental variability – leaving open

123   questions about how beneficial multi-sensor inferences are to RSSI predictions.

124   If RSSI can reliably estimate distance, it also opens the door to spatial localization by

125   inferring an animal's position in space by comparing RSSI from a mobile tag to three or more

126   fixed receivers, or "gateways." This technique, referred to as trilateration, has been widely

127   applied in automated VHF and UHF telemetry systems (Kays et al. 2011, Kluge et al. 2020,

128   Ripperger et al. 2020, Paxton et al. 2022). In settings where GPS is unavailable, imprecise, or

129   power-intensive, such as caves, dense forests, or burrows, RSSI-based localization offers a

130   lightweight alternative. Moreover, if multiple tagged individuals are localized with sufficient

131   accuracy, their relative positions can be used to reconstruct pairwise proximity networks without

132   direct tag-to-tag communication. While promising, the accuracy of RSSI-based localization may

133   be limited by signal variability. Whether integrating additional tag-measured context (*e.g.*,

134   weather or line-of-sight conditions) can improve trilateration performance remains an open

135   question.

136   As animal-borne GPS tracking continues to expand in both taxonomic breadth and global

137   scale (Kays and Wikelski 2023), there is growing interest in using GPS not only to track

138   movement but also to infer interactions between individuals (He et al. 2023, Yang et al. 2023),

139   relevant to information exchange (Merkle et al. 2024) or disease spread (Wilber et al. 2022).

140   However, GPS is accompanied by positional error, ranging from several to tens of meters

141   depending on environment (Frair et al. 2010), and variable time-to-fix delays, ranging from

142   several seconds to minutes (He et al. 2023). As a result, GPS often overestimates distance

143   between tags (He et al. 2023), possibly missing important fine-scale interactions. In contrast,

144   proximity sensing may offer time-synchronized observations (Wild et al. 2024) and greater

145 accuracy than GPS at fine spatial scales. Though, empirical comparisons are needed to evaluate

146 when and how these methods yield different conclusions about animal interactions.

147   In this study, we used the multi-sensor WildFi biologger (Wild et al. 2022b) to evaluate

148 RSSI's performance as a tool for proximity estimation (both continuous and contact-based) and

149 localization under varying conditions. We conducted three experiments and a field trial: (1)

150 testing how tag orientation affects RSSI-distance relationships (**Fig. 1A**); (2) assessing whether

151 tag-measured temperature data improves proximity estimates (**Fig. 1B**); (3) evaluating

152 trilateration using RSSI in a fixed gateway array (**Fig. 1C**); and (4) comparing GPS- and RSSI-

153 inferred proximity in free-ranging Egyptian fruit bats (*Rousettus aegyptiacus*) (**Fig. 1D**). Across

154 these tests, we asked whether RSSI alone is sufficient for fine-scale inference, and whether

155 incorporating sensor-derived covariates improved accuracy. By combining experimental

156 validation with field deployment, we assessed the value of multi-sensor biologging for proximity

157 inference in behavioral ecology.

158

159 **Materials and Methods:**

160 ***Experiment 1: RSSI and tag orientation***

161   RSSI typically decays with distance, but factors such as tag orientation can influence how

162 anisotropic signals propagate through space (Rutz et al. 2015). To test the effect of tag

163 orientation on RSSI-distance relationships, we conducted an experiment with two WildFi tags

164 placed on 1-m-high stakes at distances from 3.5 cm to 10 m, with line-of-sight between tags. We

165 recorded RSSI every minute for 10 minutes at each of five relative orientations: (1) antennae

166 facing together, (2) facing away, (3) perpendicular, (4) collinear in opposite directions, and (5)

167 collinear in the same direction.

168

Experiment 2: RSSI and tag-sensed temperature

170   Signal propagation in WiFi and other UHF systems can vary with ambient environmental

171   conditions, including air temperature (Marfievici et al. 2013). To evaluate how ambient

172   temperature influences RSSI-based distance estimates, we deployed 35 WildFi tags in arrays at

173   known distances (1 cm to 21.4 m) and uniform orientation. Tags were placed 30 cm above the

174   ground on plastic stools and recorded RSSI and onboard temperature every 30 min from 5:00–

175   20:00 across trials lasting 30 minutes to 2 days. Natural temperature variation (2.1–53.5 °C)

176   enabled assessment of temperature effects on RSSI under field conditions.

177

Experiment 3: RSSI and gateway-based trilateration

179   RSSI can be used to trilaterate mobile tags; however, obstructions can distort RSSI and

180   affect localization accuracy (Rutz et al. 2015). To test whether tag-measured temperature and

181   line-of-sight conditions influence RSSI–distance estimates and localization, we deployed 16

182   fixed WildFi gateways across six, 10.5 m × 21 m walled enclosures (**Figs S1-2**, approximately

183   1.3 ha). Tags were placed at known positions (2-15 m apart) on 30 cm-high stools and recorded

184   RSSI and temperature every 30 min from 05:00-20:00. For each tag–gateway pair, we recorded

185   whether a physical wall obstructed the signal to define a binary "line-of-sight" variable.

186

Field Trial: RSSI vs. GPS and on-animal inferences

188   While GPS error is predicted to inflate pairwise distances (He et al. 2023), it is unclear

189   whether RSSI is more accurate in pairwise distance estimation. We compared RSSI- and GPS-

190   based proximity using data on 154 free-ranging Egyptian fruit bats captured in Cyprus, fitted

191   with WildFi biologgers programmed to record RSSI, GPS locations, and environmental data

192   (temperature, relative humidity, and barometric pressure) every 5 min for approximately 5 days.

193   GPS sampling faced variable time-to-fixed intervals, ranging from 1 to 255 seconds (mean =

194   20.6 s). We minimized the effect of RSSI-GPS asynchrony by only retaining observations with

195   ≤30 s time difference between paired GPS fixes and RSSI measures. Though, thresholds up to

196   300 s did not alter inferences (**Figs S3–5**).

197

198   ***Statistical analysis***

199   We modeled tag–tag and tag–gateway distances as a function of RSSI using Gamma

200   regression models with a log-link based on fit comparisons to Gaussian and log-Gaussian

201   alternatives (**Fig. S6**). In addition to RSSI-only models, we fit more complex models

202   incorporating additional variables (tag orientation in **Experiment 1**, temperature in **Experiment**

203   **2**, line-of-sight and temperature in **Experiment 3**, and temperature, relative humidity, and

204   barometric pressure in the **Field Trial**). Random effects were included for the tag recording

205   RSSI, and where applicable, for the alternate tag or receiving gateway. All predictor variables

206   were scaled and centered prior to fitting using *glmmTMB* (Brooks et al. 2017), and we assessed

207   model fit using *DHARMa* (Hartig 2018). We evaluated nonlinear RSSI-distance relationships

208   using generalized additive models in *mgcv* (Wood 2010) (**Figs S7-9**). In the **Field Trial**, we

209   found a nonlinear relationship with GPS-inferred distance plateauing at ~48 m for RSSI values

210   greater than –75 (**Fig. S10**). To address this issue, we took two modeling approaches: first, we

211   log-transformed RSSI to capture the observed nonlinear structure in GPS-inferred distances (**Fig.**

212   **S11**); second, we alternatively excluded observations with RSSI values > -75, reducing the

213   influence of potential GPS error. Under this filtering approach, the relationship between RSSI

214 and distance more closely resembled the linear exponential decay pattern observed in

215 **Experiments 1–3** (**Fig. S12**).

216   We assessed model performance based on (1) model fit and (2) predictive accuracy on

217 out-of-sample data. First, we compared RSSI-only and more complex model fit using Akaike's

218 Information Criterion (AIC), with differences >4 indicating strong support for the more complex

219 model (Akaike 1998). We also calculated marginal and conditional R^2 of models estimated using

220 *MuMIn* (Barton 2009). Second, we evaluated predictive performance using cross-validations

221 with 25 random splits into training (75%) and testing (25%) data. We generated predictions both

222 conditioned on tag/gateway identity and using only population-level effects (i.e., as if there were

223 no pre-deployment validation data). We evaluated predictive error based on continuous distance

224 predictions (using median R^2 and root mean squared error [RMSE]) and accuracy in classifying

225 contact, based on multiple distance thresholds. We compared accuracy against a random

226 classifier determined by the proportion of true "contacts" at various distance thresholds in testing

227 data (p), with accuracy equal to $p^2+(1-p)^2$. We additionally report sensitivity and specificity in

228 **Figs S13-16**.

229

230 *Trilateration positional accuracy inferred proximity networks*

231   We tested whether RSSI-based trilateration could accurately localize tags and reconstruct

232 proximity networks within gateway arrays. Using nonlinear least squares (NLS) regression based

233 on previous trilateration approaches (Paxton et al. 2022), we estimated tag positions based on

234 predicted distances to fixed WiFi gateways with known locations. For each tag and time point,

235 we used all gateways observed by a tag (mean = 13.097, range: 10-15) and generated two types

236 of predictions: (1) conditional on tag-specific random effects, or (2) using only population-level

237 effects. To account for the expected increase in error with weaker RSSI, we assigned

238 exponentially decaying weights to tag–gateway distance predictions, and we initialized NLS

239 models with start locations based on the weighted average of all gateway coordinates. We

240 quantified Euclidean error of location estimates, and we compared correlations between

241 trilateration-inferred and true proximity networks.

242

243 ***RSSI- vs. GPS-inferred proximity and contact networks***

244 We compared RSSI- and GPS-inferred proximity networks using data from free-flying

245 bats. Using predictions from the top **Field Trial** model (based on a dataset filtered to RSSI ≤ -

246 75), we constructed (1) continuous networks based on average pairwise distances, and (2) binary

247 contact networks at thresholds from 0.5-500 m. We generated equivalent networks from GPS by

248 computing pairwise distances for GPS fixes. We compared the correlation between respective

249 distance and contact networks using Mantel tests in *vegan* (Oksanen et al. 2013).

250 We assessed whether discrepancies between RSSI and GPS were driven by GPS error by

251 simulating positional error from gamma distributions fit to empirical GPS data (Wild et al.

252 2022a) (**Figs S13-19**). We generated 1,000 replicate GPS position pairs for true distances

253 ranging from 0.01-1,000 m, incorporating stochastic error into each fix, and calculated apparent

254 inter-tag distances. We compared simulated GPS distances to empirical RSSI estimates and

255 calculated percent error across distances. This allowed us to assess whether observed divergence

256 between GPS and RSSI proximity was consistent with expected GPS error and how it compared

257 to known RSSI error from **Experiments 1-3**. We performed all analyses using Program R

258 version 4.3.2 (Team 2021).

259

260   **Animal Handling:**

261   Data from Egyptian fruit bats were collected with ethical permission from the Ministry of

262   Agriculture, Agricultural Development and Environment, Cyprus, under permit numbers

263   02.15.001.003/04.05.002.005.006/02.15.007.003.002 (10/10/2022).

264

265   **Results:**

266   ***Experiment 1: RSSI and tag orientation***

267   We first tested whether tag orientation affected the relationship between RSSI and

268   distance. Using a controlled setup with two tags spaced from 3.5 cm to 10 m, we found that tag

269   orientation significantly influenced RSSI across all distances (likelihood ratio test [LRT] $\chi^2 =$

270   1859, df = 4, p-value < 0.001; **Fig. 2A, Table 1**). Full models including orientation were favored

271   over RSSI-only models based on AIC comparisons, and full models explained more variance in

272   observed data (conditional $R^2 = 0.963$, marginal $R^2 = 0.963$) than RSSI-only models (conditional

273    $R^2 = 0.800$, marginal $R^2 = 0.800$, **Table 1**). Even without information about orientation, RSSI

274   alone was a strong predictor of tag-tag proximity (β = -1.746, standard error [SE] = 0.031; LRT

275    $\chi^2 = 3227$, df = 1, p-value < 0.001, **Table 1**).

276   In cross-validations, full models including orientation (median $R^2 = 0.833$, median RMSE

277   = 1.36 m) outperformed RSSI-only models (median $R^2 = 0.503$, median RMSE = 3.87 m, **Table**

278   **S1**). Continuous prediction error tended to increase proportionately with true distance, but

279   orientation-informed models maintained lower error throughout yielding a median error of 11 cm

280   at 1 m, 1.90 m at 5 m, and 2.43 m at 10 m (**Fig. 2B**). Classifications of contact based on different

281   distance thresholds also favored full models including orientation over RSSI only models (**Fig.**

282   **2C, Fig. S13**). Yet, both RSSI-only and full models performed better than a random classifier

283   with median accuracy greater than 82.5% and 87.5% across all distance thresholds, respectively

284   (**Fig. 2C**). These results confirm that tag orientation introduces meaningful signal variation, but

285   that RSSI alone can still yield reasonably accurate proximity estimates in the face of variation in

286   tag orientations.

287

288   ***Experiment 2: RSSI and tag-sensed temperature***

289   We next tested whether tag-sensed ambient temperature influenced the relationship

290   between RSSI and distance. Using 25 tags spaced from 1 cm to 21.5 m, we found that

291   temperature had a significant effect on predicted distance, accounting for RSSI (β = -0.178, SE =

292   0.001, LRT χ^2 = 32801, df = 1, p-value < 0.001, **Fig. 3A, Table 2**). Models including

293   temperature were also favored over RSSI-only models based on AIC comparisons and explained

294   more variation in the observed data (conditional R^2 = 0.836, marginal R^2 = 0.728) than RSSI-

295   only models (conditional R^2 = 0.814, marginal R^2 = 0.704, **Table 2**). Tag-level random effects

296   were important in RSSI variation, explaining approximately 10–11% of variation. Notably, RSSI

297   alone was a strong predictor of pairwise distances, even when ambient weather conditions were

298   unaccounted for (β = -1.093, SE = 0.001, LRT χ^2 = 1035446, df = 1, p-value < 0.001).

299   Cross-validations confirmed that models including temperature produced more accurate

300   predictions (median R^2 = 0.697, median RMSE = 1.894 m) than RSSI-only models (median R^2 =

301   0.585, median RMSE = 2.721 m, **Table S2**). Prediction errors increased with true distance: for

302   example, the top model produced median error of 34.2 cm at distances <1 m, 59.9 cm at 2.2-3 m,

303   and 1.67 m at 5-7.5 m (**Fig. 3B**). Contact classification also favored models including

304   temperature over RSSI-only models, but all models outperformed a random classifier (**Fig. 3C,**

305   **Fig. S14**). Conditioned on tag identity, contact classification accuracy was >80.6% across all

306   distance thresholds; in contrast, predictions assuming population-level averages was only

307   >72.9% accuracy. Fine-scale contacts were exceptionally accurate with approximately 95%

308   accuracy in defining contacts <1 m (**Fig. 3C**). These results demonstrate that RSSI can provide

309   effective proximity estimates, and that accounting for tag-sensed temperature or tag-level

310   heterogeneity can further improve performance.

311

312   ***Experiment 3: RSSI and tag-gateway communications***

313   We then tested whether tag-measured temperature or information about gateway

314   positioning (specifically, line-of-sight conditions) could increase the predictive performance of

315   RSSI in tag-gateway distance estimates. Across 16 fixed gateways and a range of tag positions

316   within a 64 m × 21 m enclosure, we found that tag-measured temperature affected distance

317   estimates (β = -0.022, SE = 0.001, LRT χ^2 = 58.3, df = 1, *p*-value < 0.001), and that line-of-sight

318   obstructions affected the relationship between RSSI and true distance (LRT χ^2 = 1187.8, df = 1,

319   *p*-value < 0.001, **Fig. 4A, Table 3**). Models included both tag-measured temperature and an

320   interaction between RSSI and line-of-sight were favored over RSSI-only models in AIC

321   comparisons and explained substantially more variation in distance estimates (conditional R^2 =

322   0.850, marginal R^2 = 0.692) than RSSI-only models (conditional R^2 = 0.771, marginal R^2 =

323   0.567, **Table 3**). Tag and gateway random effects explaining approximately 15-20% of variation

324   in distance predictions, indicating a significant role of device variation. When line-of-sight

325   conditions or tag-measured temperature were unaccounted for, RSSI alone remained a strong

326   predictor of distance (β = -0.490, SE = 0.006, 95% CI; LRT χ^2 = 5955, df = 1, *p*-value < 0.001).

327   In out-of-sample predictions, the full model yielded more accurate distance estimates

328   (median R^2 = 0.838, median RMSE = 3.28 m) than RSSI-only models (median R^2 = 0.794,

329   median RMSE = 3.78 m, **Table S3**). Prediction error was relatively small compared to true

330   distance, with the top model producing median error of 1.25 m between 5.34 - 8.91 m, 2.36 m

331   between 17 - 19 m, and 2.00 m between 24.7 - 28.4 m. Full models also classified contacts more

332   accurately than RSSI-only models, but all models outperformed a random classifier with greater

333   than 73.3-83% accuracy across all distances (**Fig. 4C**, **Fig. S15**).

334

335   *RSSI-Based trilateration using gateway arrays*

336   We next evaluated whether RSSI-based distance estimates could be used to localize tags

337   via trilateration. Using nonlinear least squares trilateration, we estimated a median positional

338   error of 2.59 m (95% interval: 0.560 – 6.04 m) for the full model (including tag-measured

339   temperature and an interaction between RSSI and line-of-sight), and 3.02 m (95% interval: 0.588

340   – 7.08 m) for the RSSI-only model, conditional on tag-level random effects (**Fig. 5A**, **Fig. S17**).

341   When using population-level predictions, we found roughly similar error for the full model

342   (median = 2.56 m; 95% interval: 0.558 – 6.56 m) but slightly higher error for the RSSI-only

343   model (median = 3.29 m; 95% interval: 0.836 – 7.03 m, **Fig. 5A**).

344   All trilateration-based networks were strongly correlated with the ground-truth proximity

345   networks, though the strength of this correlation varied by model structure. Networks derived

346   from the full model had slightly higher correlations (median = 0.725, 95% interval = 0.150 –

347   0.942) than those based on RSSI alone (median = 0.672, 95% interval = 0.104 – 0.920), when

348   conditioned on tag identity (**Fig. 5B**, **Fig. S18**). Removing tag-level random effects slightly

349   reduced correlations for both the more complex model (median = 0.606, 95% interval = 0.353 –

350   0.928) and the RSSI-only model (median = 0.542, 95% interval = 0.291 – 0.907, **Fig. 5B**). These

351   results suggest that RSSI-based inferences in gateway arrays can provide reasonably accurate tag

352   locations useful in generating indirect pairwise proximity estimates.

353

354   ***Field Trial: RSSI vs. GPS and on-animal inferences***

355   Finally, we sought to understand how RSSI-based distance predictions compared to GPS-

356   based proximity. Using paired RSSI and GPS data from 154 free-flying Egyptian fruit bats, we

357   found that RSSI was associated with GPS-inferred pairwise distances both when RSSI was log-

358   transformed to address non-linearity in the relationship between RSSI-GPS distance (β = -0.549,

359   SE = 0.016, LRT χ^2 = 1113.8, df = 1, *p*-value < 0.001, **Table 4**), as well as when the dataset was

360   filtered to RSSI-GPS observations less likely to be affected by GPS positional error (β = -0.375,

361   SE = 0.019, LRT χ^2 = 399.71, df = 1, *p*-value < 0.001, **Table 5**). Under both modeling

362   approaches, we found that models including RSSI and tag-measured temperature, relative

363   humidity, and atmospheric pressure were favored over RSSI-only models (**Fig. 6A**, **Tables 4-5**).

364   Cross-validations using all paired RSSI and GPS data showed that including additional

365   tag-measured weather data generated slightly more accurate out-of-sample predictions (median

366   R^2 = 0.239, median RMSE = 169.280 m) than RSSI-only models (median R^2 = 0.232, median

367   RMSE = 169.415 m, **Table S4**). Distinct from **Experiments 1-3**, prediction error decreased with

368   GPS-inferred distances until approximately 45 m but increased gradually for distances beyond 45

369   m (**Fig. 6B**). In the top model, for example, median differences between RSSI- and GPS-inferred

370   distances were 41.2 m, 24.7 m, and 58.0 m for GPS-inferred distance bins of 0-15.8 m, 33.9-44.1

371   m, and 134-244 m, respectively. Full models including tag-measured weather classified GPS-

372   inferred contacts with similar accuracy to RSSI-only models (**Fig. 6B**, **Fig. S16**). While models

373   generally outperformed a random classifier, accuracy was much lower than in **Experiments 1-3**

374   (**Fig. 6C**).

375

376   ***RSSI- vs. GPS-inferred proximity and contact networks***

377   Using a model excluding observations with RSSI >-75 (where GPS positional error may

378   have been large relative to true pairwise distances), we compared GPS- and RSSI-inferred

379   proximity networks. Across all distances, RSSI- and GPS-inferred average pairwise distance

380   networks were correlated (Mantel statistic r = 0.603, p-value = 0.001, **Fig. 7A**). However, at

381   close range (<100 m), this relationship disappeared (Mantel statistic r = 0.296, p-value = 0.135),

382   suggesting divergence in fine-scale proximity estimates (**Fig. 7C**). In total contact networks, we

383   found that RSSI and GPS inferences were unrelated for contacts definitions <5 m, weakly

384   correlated for contacts definitions between 5-25 m, and relatively strongly correlated for contact

385   definitions >50 m (**Fig. 7D**). For example, RSSI- and GPS-inferred 5 m contact networks are

386   largely uncorrelated with each other (**Fig. 7B**).

387   Simulated GPS data, generated using a gamma distribution fit to empirical chip error

388   (**Figs S19-21**), showed consistent overestimation of true distances <50 m, matching observed

389   discrepancies between GPS and RSSI (**Fig. 7C**). Comparisons of percent error showed that GPS

390   consistently overestimated close-range proximity (<50 m) relative to true distances, with higher

391   error than RSSI-based estimates from **Experiments 1–3** (**Fig. S22**). These results suggest a

392   tradeoff in the accuracy of RSSI- and GPS-based inferences, with RSSI potentially out-

393   performing GPS at pairwise distances <50 m.

394

395   **Discussion:**

396   Accurately quantifying spatial proximity is central to understanding social behavior,

397   information flow, and pathogen transmission in animals (Krause et al. 2013, Smith and Pinter-

398   Wollman 2021, Suraci et al. 2022). Here, we used a series of controlled experiments and field

399   trials with multi-sensor WildFi biologgers (Wild et al. 2022b) to evaluate the utility of WiFi-

400   based RSSI as a continuous proxy for proximity and localization. We found that RSSI can

401   produce biologically useful estimates of distance, outperform GPS at close range, and support

402   trilateration over narrow spatial extents. Across applications augmenting RSSI with tag-

403   measured environmental data, other contextual data, and information about tag variation

404   significantly benefited inferences.

405   RSSI was an effective proxy for pairwise distance, with conditional R^2 values of 0.771 -

406   0.936 across experiments. Out-of-sample cross-validations supported RSSI as an effective tool

407   for predicting proximity in new contexts, with median error often <50% of the true distance and

408   exceptional contact classification accuracy (>85-95%) for pairwise distances <2 m. However,

409   our work also echoes previous findings, showing that RSSI is influenced by tag orientation,

410   weather, obstructions, and tag variation (Prange et al. 2006, Böhm et al. 2009, Drewe et al. 2012,

411   Boyland et al. 2013, Marfievici et al. 2013, Bettaney et al. 2015, Rutz et al. 2015). Building from

412   previous work, we highlight how multi-sensor data can be used to refine RSSI-based inferences.

413   Specifically, tag-measured temperature was universally favored by AIC and modestly increased

414   R^2 by 1-3%. Our findings also reinforce the importance of context-specific calibration (Rutz et

415   al. 2015), with 10-20% of variation in distance often resulting from tag random effects. While

416   RSSI alone can serve as an effective proxy, pre-deployment validations and tag-measured data

417   provide substantial performance gains with richer behavioral inference than RSSI alone.

418   Given the predictive accuracy of RSSI, we could trilaterate tag locations within a 1.3 ha

419   gateway array with median Euclidean error of 2.6-3.3 m, accurate enough to reconstruct

420   proximity networks. Including line-of-sight conditions, tag-measured temperature, and tag

421   random effects further improved localization accuracy and network correlations. Compared to

422   RFID arrays, which are limited to point detections, and GPS, which may be unavailable, too

423   energy intensive, or too imprecise in some systems, RSSI trilateration offers a compelling middle

424   ground – providing continuous spatial estimates over narrow spatial extents with lower noise and

425   fewer outliers. While performance will vary with gateway layout and density (Kluge et al. 2020,

426   Ripperger et al. 2020), these findings suggest that RSSI can make localization and indirect

427   spatial interactions viable for behavioral inferences.

428   In free-ranging Egyptian fruit bats, RSSI was correlated with GPS-inferred distances but

429   with greater variability than in controlled settings. While RSSI remained predictive across a

430   broad range (up to 250 m), its relationship with GPS was nonlinear and noisier - partially

431   reflecting positional uncertainty in the GPS data itself. Simulations using empirical GPS error

432   confirmed that GPS systematically overestimated close-range distances (<50 m) as shown by He

433   et al. (2023), consistent with divergence between RSSI- and GPS-based proximity networks at

434   these scales. As a result, GPS and RSSI were weakly correlated (if at all) at distances <50 m,

435   suggesting that GPS and RSSI differ most at the short ranges biologically relevant to

436   epidemiological contact or direct social interaction. Interestingly, RSSI and GPS estimates were

437   relatively well-correlated at intermediate-to-longer ranges (100-250 m), suggesting that some

438   RSSI signals may also capture broader-scale spatial associations. There is increasing interest in

439   the fine-scale interactions shaping animal societies and epidemiology through GPS tracking

440   (Manlove et al. 2022, Wilber et al. 2022, He et al. 2023, Yang et al. 2023). Our findings

441   highlight the importance of matching tools to the spatial and temporal scale of interest. For

442   quantifying contacts or social structure within groups, RSSI may offer better resolution and

443   lower bias than GPS. Used together, these technologies can provide complementary views of

444   animal space use, proximity, and interaction across scales.

445   Our results demonstrate that RSSI is a practical and scalable tool for estimating fine-scale

446   animal proximity and localization, particularly in conditions where GPS may fail. Rather than

447   treating RSSI variability as noise, we show that environmental context and tag-specific effects

448   can be leveraged to refine inference and move beyond binary contact definitions. This echoes

449   calls for rigorous pre-deployment validation and context-specific calibration (Rutz et al. 2015),

450   and we suggest that factors like ambient weather conditions should be considered when

451   designing validation experiments. Importantly, our work also suggests that multi-sensor

452   biologgers can help refine RSSI proximity sensing by capturing variation in ambient weather.

453   Multi-sensor platforms are rapidly evolving and can accommodate many more data streams than

454   weather alone (Williams et al. 2020). Including additional sensors (*e.g.*, accelerometers,

455   magnetometers) on tags offers exciting opportunities to possibly further resolve behavioral

456   effects on RSSI, accounting for the effects of motion, orientation, or other tag contexts.

457   Synthesizing multiple data streams alongside RSSI can also offer avenues for edge computing

458   (Yu et al. 2024) to create modeled "virtual sensors" of pairwise distance on tags that reduce data

459   transmission costs and preserve biological inferences. More broadly, RSSI enables both accurate

460   proximity sensing and trilateration, offering a powerful framework for high-resolution inference

461   of animal interactions, advancing our ability to study social behavior in the wild.

462

463 **Tables:**

464 **Table 1:** Summaries and comparison of generalized linear mixed-effect models of known

465 distance based on RSSI and orientation from **Experiment 1** with Gamma log-link function (n_{tags}

466 = 2, $n_{observations}$ = 800). Estimates are on link scale with standard error in parentheses. Stars denote

467 p-values with: * p-value $\leq$ 0.05, ** p-value $\leq$ 0.01, *** p-value $\leq$ 0.001.

	Null	Orientation
Intercept	-0.107 (0.027)***	0.418 (0.038)***
RSSI	-1.746 (0.031)***	-1.891 (0.016)***
Collinear, Same Direction		0.103 (0.049)*
Facing Away		-0.978 (0.049)***
Facing Together		-1.597 (0.049)***
Perpendicular		-1.221 (0.05)***
Focal ID Random Effect SD	1.29e-05	2.07e-02
ΔAIC	968.1028	0
Conditional R^2	0.800	0.936
Marginal R^2	0.800	0.936

468

469   **Table 2:** Summaries and comparison of generalized linear mixed-effect models of known

470   distance based on RSSI and tag-measured temperature from **Experiment 2** with Gamma log-link

471   function (n_{tags} = 35, $n_{observations}$ = 269,443). Estimates are on link scale with standard error in

472   parentheses. Stars denote p-values with: * p-value ≤ 0.05, ** p-value ≤ 0.01, *** p-value ≤

473   0.001.

474

	Null	Temperature
Intercept	1.055 (0.074)***	1.039 (0.073)***
RSSI	-1.093 (0.001)***	-1.097 (0.001)***
Temperature		-0.178 (0.001)***
Focal ID Random Effect SD	3.24e-01	3.20e-01
Alternate ID Random Effect SD	2.88e-01	2.86e-01
ΔAIC	31067.12	0
Conditional R^2	0.704	0.728
Marginal R^2	0.814	0.836

475

476   **Table 3:** Summaries and comparison of generalized linear mixed-effect models of known

477   distance based on RSSI and tag-measured temperature and line-of-sight conditions from

478   **Experiment 3** with Gamma log-link function ($n_{tags} = 17$, $n_{gateways} = 16$, $n_{observations} = 10,732$).

479   Estimates are on link scale with standard error in parentheses. Stars denote p-values with: * p-

480   value ≤ 0.05, ** p-value ≤ 0.01, *** p-value ≤ 0.001.

	Null	*Temperature*	*Line of Sight*	*Line of Sight Interaction*	*Line of Sight Interaction and Temperature*
Intercept	2.751 (0.08)***	2.746 (0.078)***	2.893 (0.078)***	3.036 (0.074)***	3.028 (0.073)***
RSSI	-0.49 (0.006)***	-0.503 (0.006)***	-0.478 (0.006)***	-0.21 (0.01)***	-0.224 (0.01)***
Temperature		-0.028 (0.003)***			-0.022 (0.003)***
Line-of-Sight (vs. Blocked)			-0.356 (0.026)***	-0.403 (0.026)***	-0.397 (0.026)***
RSSI* Line-of-Sight				-0.389 (0.011)***	-0.385 (0.011)***
Focal ID Random Effect SD	8.17E-02	8.20E-02	7.91E-02	6.77E-02	6.81E-02
Gateway:Year Random Effect SD	2.69E-01	2.70E-01	2.44E-01	2.80E-01	2.83E-01
Year Random Effect SD	8.34E-02	7.91E-02	8.27E-02	6.80E-02	6.39E-02
ΔAIC	1394.48	1312.19	1210.31	56.06	0
Conditional R^2	0.567	0.579	0.691	0.689	0.692
Marginal R^2	0.771	0.778	0.825	0.847	0.85

481

482   **Table 4:** Trial with Gamma log-link function and log-transformed RSSI.

483   Summaries and comparison of generalized linear mixed-effect models of GPS-inferred distance

484   based on RSSI and tag-measured weather data from the **Field Trial** on with Gamma log-link

485   function (n_{tags} = 136, $n_{gateways}$ = 136, $n_{observations}$ = 2,948). Estimates are on link scale with standard

486   error in parentheses. Stars denote p-values with: * p-value $\leq$ 0.05, ** p-value $\leq$ 0.01, *** p-value

487    $\leq$ 0.001.

	Null	Temperature	Humidity	Pressure	All Weather
Intercept	4.679 (0.046)***	4.673 (0.046)***	4.687 (0.046)***	4.666 (0.046)***	4.669 (0.045)***
Log(RSSI+97)	-0.549 (0.016)***	-0.549 (0.016)***	-0.549 (0.016)***	-0.548 (0.016)***	-0.549 (0.016)***
Temperature		-0.029 (0.018)			-0.045 (0.019)*
Humidity (%)			-0.063 (0.021)**		-0.079 (0.022)***
Pressure (hPa)				-0.066 (0.026)*	-0.059 (0.026)*
Focal ID Random Effect SD	3.14e-01	3.13e-01	3.16e-01	3.08e-01	3.09e-01
Alternate ID Random Effect SD	3.13e-01	3.11e-01	3.10e-01	3.13e-01	3.03e-01
ΔAIC	14.94187	14.28699	7.967	10.59655	0
Conditional R^2	0.228	0.229	0.23	0.228	0.233
Marginal R^2	0.377	0.376	0.378	0.375	0.375

488

489 **Table 5:** Summaries and comparison of generalized linear mixed-effect models of GPS-inferred

490 distance based on RSSI and tag-measured weather data from the **Field Trial** on with Gamma

491 log-link function, removing observations with RSSI >-75 (n_{tags} = 134, $n_{gateways}$ = 134, $n_{observations}$ =

492 2,144). Estimates are on link scale with standard error in parentheses. Stars denote p-values with:

493 * p-value ≤ 0.05, ** p-value ≤ 0.01, *** p-value ≤ 0.001.

|	Null	Temperature	Humidity	Pressure	All Weather
Intercept	4.96 (0.054)***	4.951 (0.054)***	4.967 (0.054)***	4.941 (0.054)***	4.94 (0.053)***
RSSI	-0.375 (0.019)***	-0.378 (0.019)***	-0.375 (0.019)***	-0.375 (0.019)***	-0.379 (0.019)***
Temperature		-0.035 (0.021)			-0.047 (0.022)*
Humidity (%)			-0.052 (0.024)*		-0.068 (0.025)**
Pressure (hPa)				-0.084 (0.028)**	-0.076 (0.028)**
Focal ID Random Effect SD	3.57E-01	3.55E-01	3.58E-01	3.52E-01	3.51E-01
Alternate ID Random Effect SD	3.85E-01	3.81E-01	3.82E-01	3.82E-01	3.72E-01
ΔAIC	12.107814	11.331042	9.393676	5.03626	0
Conditional R2	0.118	0.12	0.122	0.122	0.128
Marginal R2	0.349	0.348	0.351	0.349	0.348

494
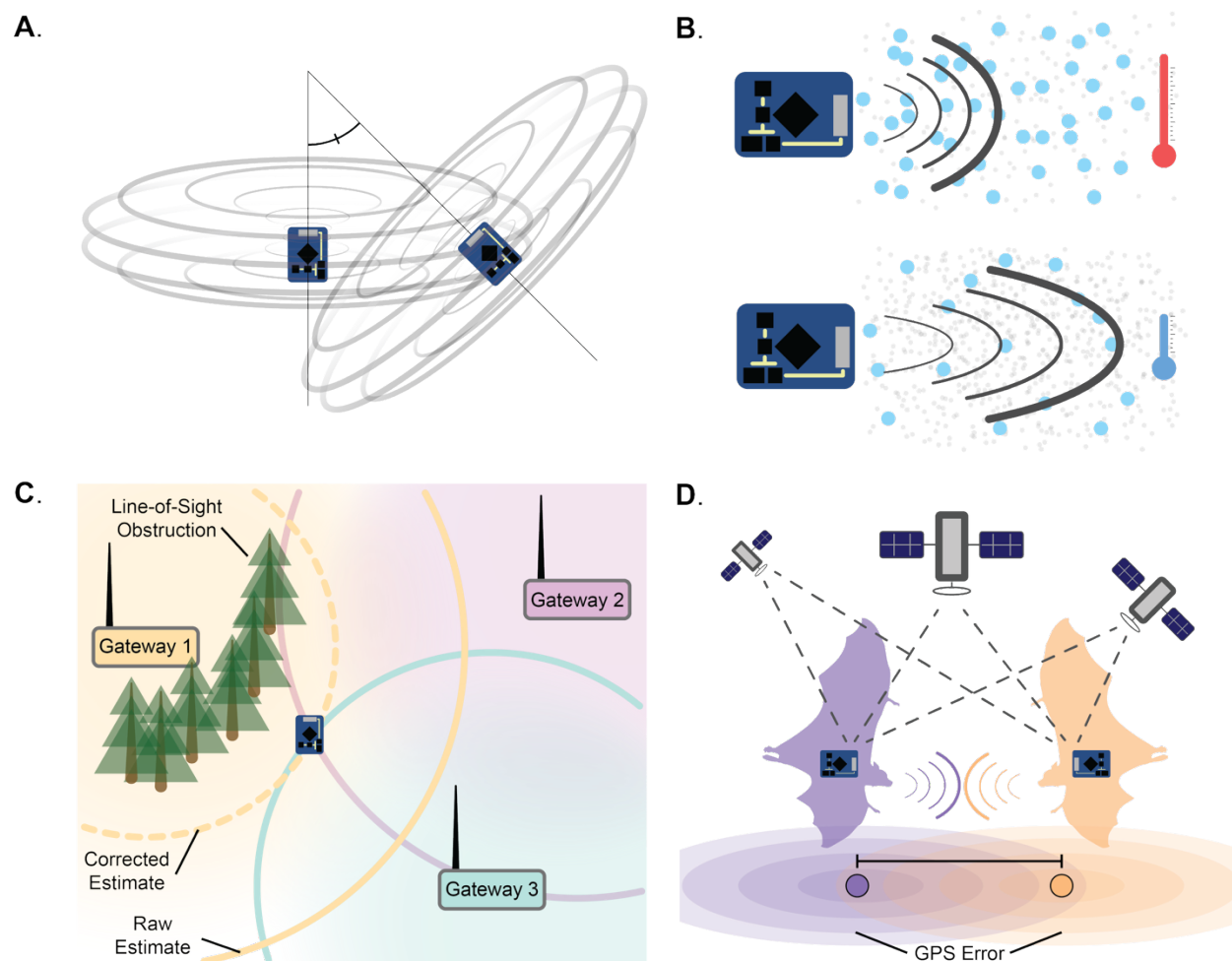
Figures:

Figure 1: **Challenges and applications in proximity sensing addressed by experiments and field trials**.

(A) Differences in tag orientation influence signal propagation, altering the relationship between Received Signal Strength Indicator (RSSI) and true distance. (B) Local weather conditions, such as temperature, humidity, and air pressure, affect air density and refractive properties, causing signal attenuation. (C) Stationary arrays enable signal localization through trilateration, though array design and obstructions may impact accuracy. (D) GPS and RSSI can both be used for proximity sensing, but GPS error may compromise fine-scale proximity estimates.
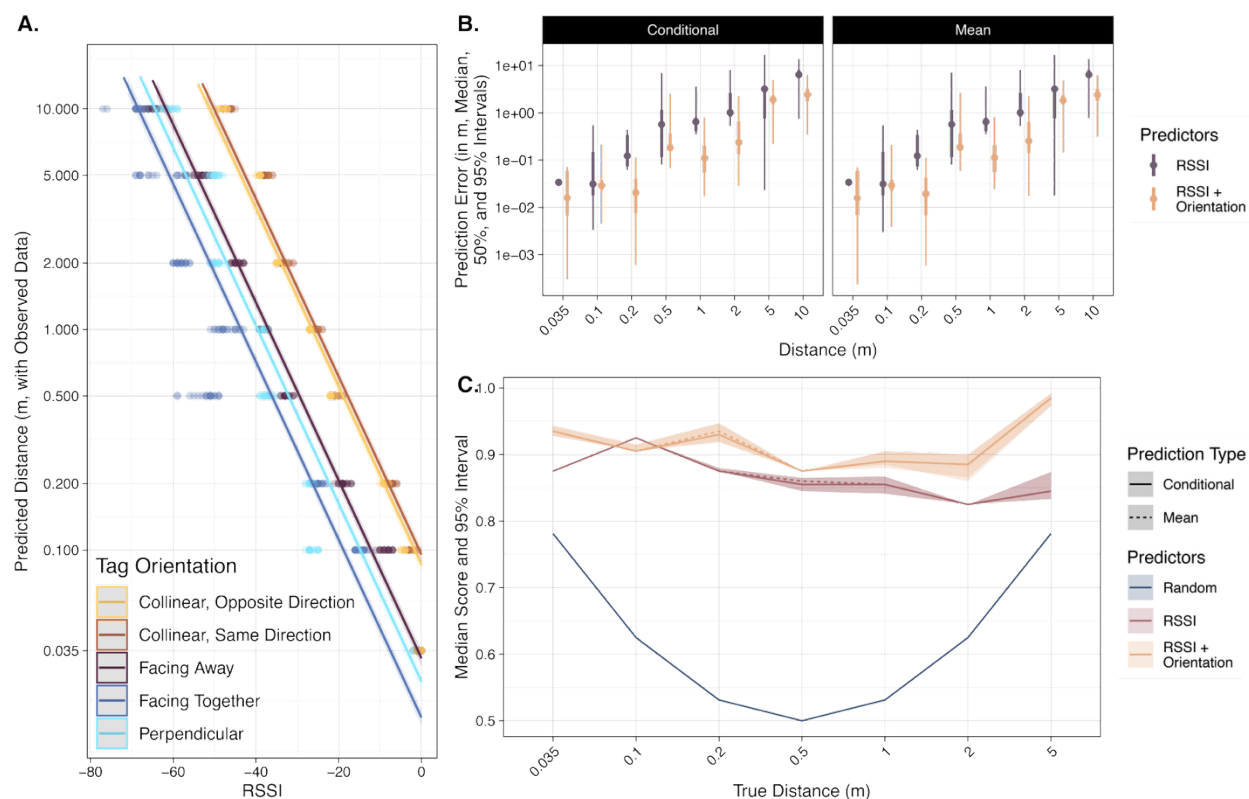
Figure 2: Effect of orientation on RSSI performance in Experiment 1.

(A) RSSI-distance relationships differ based on tag orientation (color). Shown are observed data, model estimates, 95% confidence intervals. (B) RSSI predictive error is generally lower for predictions including orientation, and error increases with pairwise distance. Shown are median, 50%, and 95% intervals of out-of-sample prediction error from cross-validations. Facets compare predictions conditioned on tag-level random effects and versus population-level average predictions. (C) Median and 95% intervals for model accuracy in classifying tag-tag communications at or below various true distance thresholds. Solid lines represent metrics based on predictions incorporating tag-level random effects, while dashed lines reflect population-only main effects. Metrics for a random classifier (blue) are also included for comparison, derived from the proportion of true contacts at each threshold.
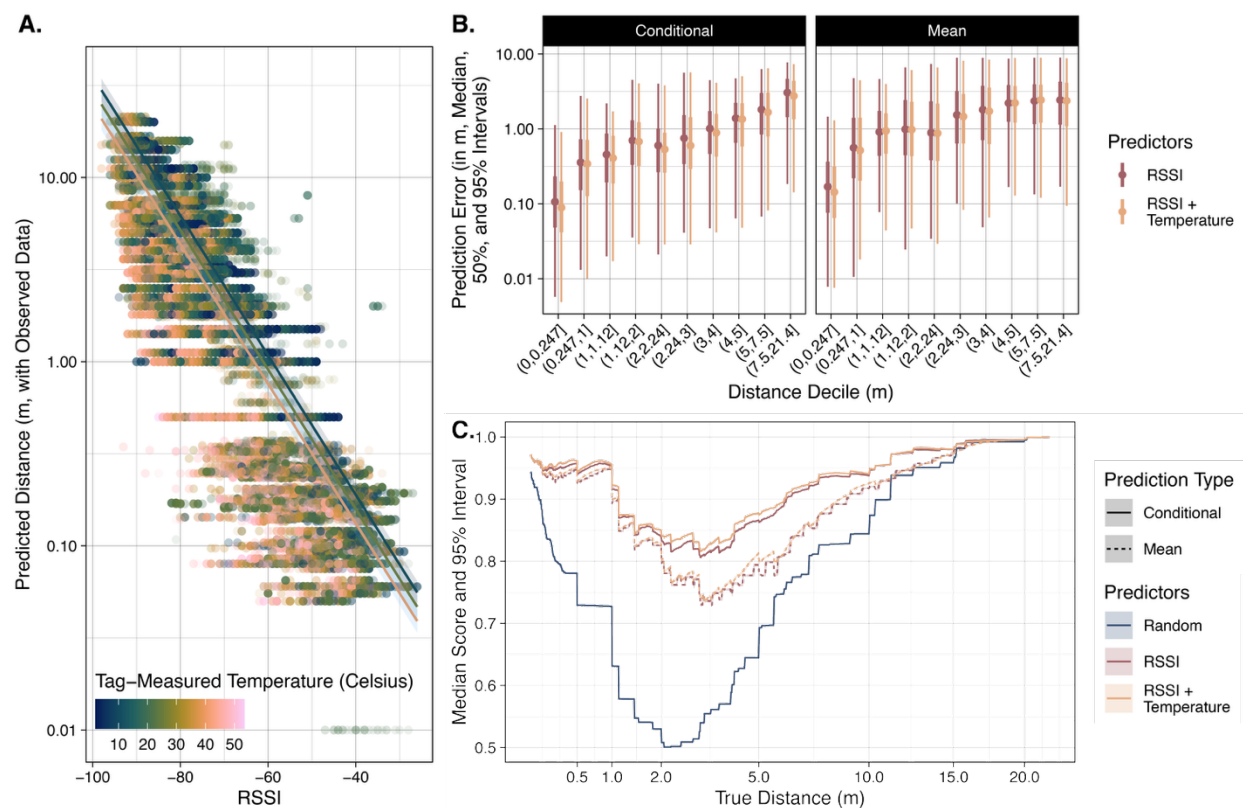
Figure 3: Effect of weather conditions on RSSI performance in Experiment 2.

(A) RSSI-distance relationships differ based on tag-measured temperature (color). Shown are observed data, model estimates, 95% confidence intervals. (B) RSSI predictive error is slightly lower for predictions including tag-measured temperature, and error increases with pairwise distance. Shown are median, 50%, and 95% intervals of out-of-sample prediction error from cross-validations. Facets compare predictions conditioned on tag-level random effects and versus population-level average predictions. (C) Median and 95% intervals for model accuracy in classifying tag-tag communications at or below various true distance thresholds. Solid lines represent metrics based on predictions incorporating tag-level random effects, while dashed lines reflect population-only main effects. Metrics for a random classifier (blue) are also included for comparison, derived from the proportion of true contacts at each threshold.
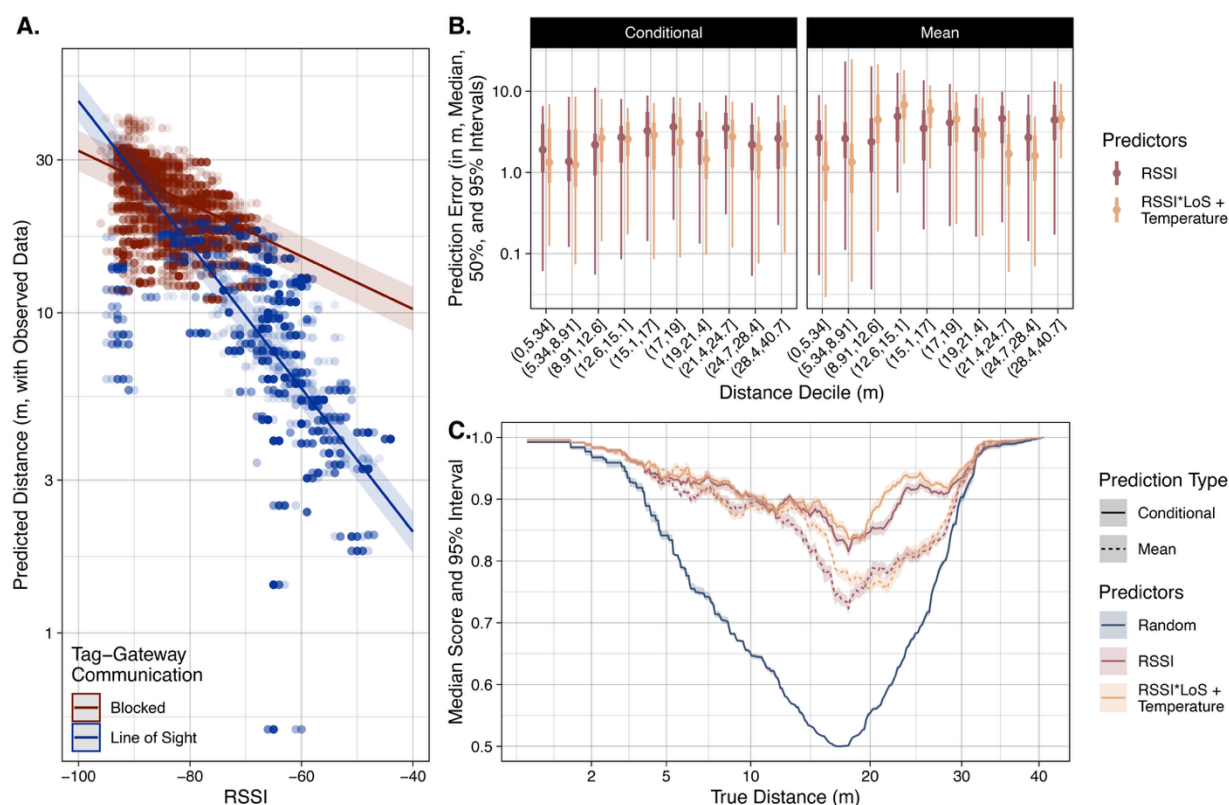
Figure 4: Effect of gateway array design on RSSI performance in Experiment 3.

(A) RSSI-distance relationships differ based on line-of-sight conditions (color). Shown are observed data, model estimates, 95% confidence intervals. (B) RSSI predictive error is generally lower for predictions including RSSI-by-line-of-sight (LoS) interactions and tag-measured temperature. Shown are median, 50%, and 95% intervals of out-of-sample prediction error from cross-validations. Facets compare predictions conditioned on tag-level random effects and versus population-level average predictions. (C) Median and 95% intervals for model accuracy in classifying tag-tag communications at or below various true distance thresholds. Solid lines represent metrics based on predictions incorporating tag-level random effects, while dashed lines reflect population-only main effects. Metrics for a random classifier (blue) are also included for comparison, derived from the proportion of true contacts at each threshold.
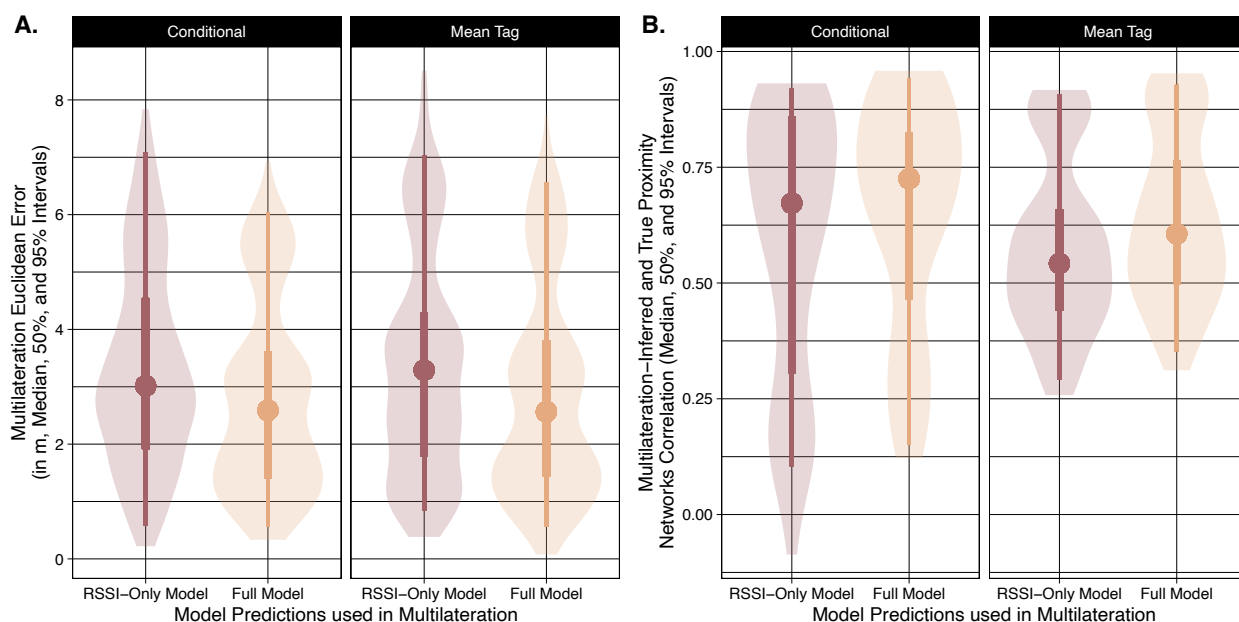
Figure 5: RSSI-based trilateration error in Experiment 3.

(A) Euclidean error in trilateration-inferred tag locations within gateway arrays compared to true locations, using an RSSI-only model and a full model incorporating RSSI, line-of-sight conditions, gateway positioning, and tag-measured temperature. (B) Correlation between trilateration-inferred and true pairwise distance networks, comparing trilateration based on RSSI-only versus full model predictions. Facets compare predictions conditioned on tag-level random effects and versus population-level average predictions.
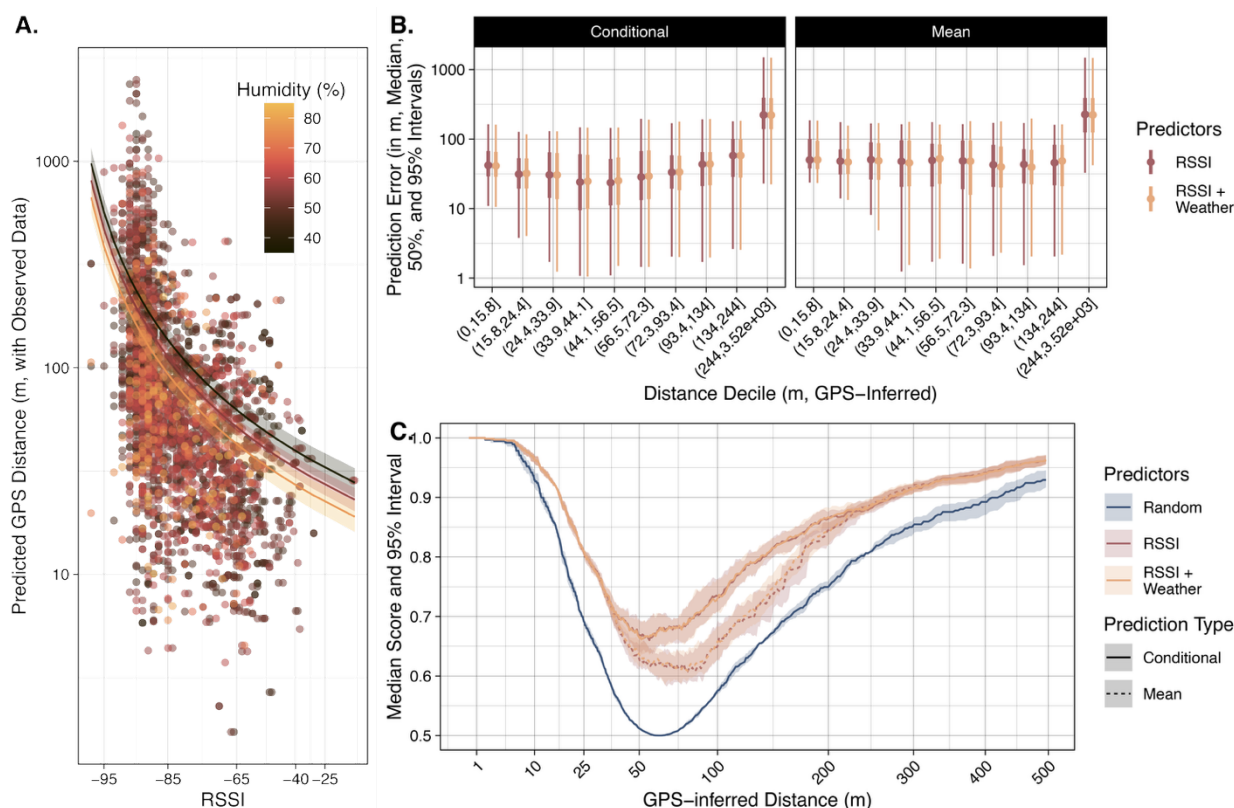
Figure 6: Effect of weather conditions on RSSI performance in the Field Trial.

(A) RSSI-distance relationships differ based on relative humidity (color). Shown are observed data, model estimates, 95% confidence intervals. (B) RSSI predictive error is generally lower for predictions including tag-measured weather data (temperature, humidity, and pressure). Shown are median, 50%, and 95% intervals of out-of-sample prediction error from cross-validations. Facets compare predictions conditioned on tag-level random effects and versus population-level average predictions. (C) Median and 95% intervals for model accuracy in classifying tag-tag communications at or below various true distance thresholds. Solid lines represent metrics based on predictions incorporating tag-level random effects, while dashed lines reflect population-only main effects. Metrics for a random classifier (blue) are also included for comparison, derived from the proportion of true contacts at each threshold.
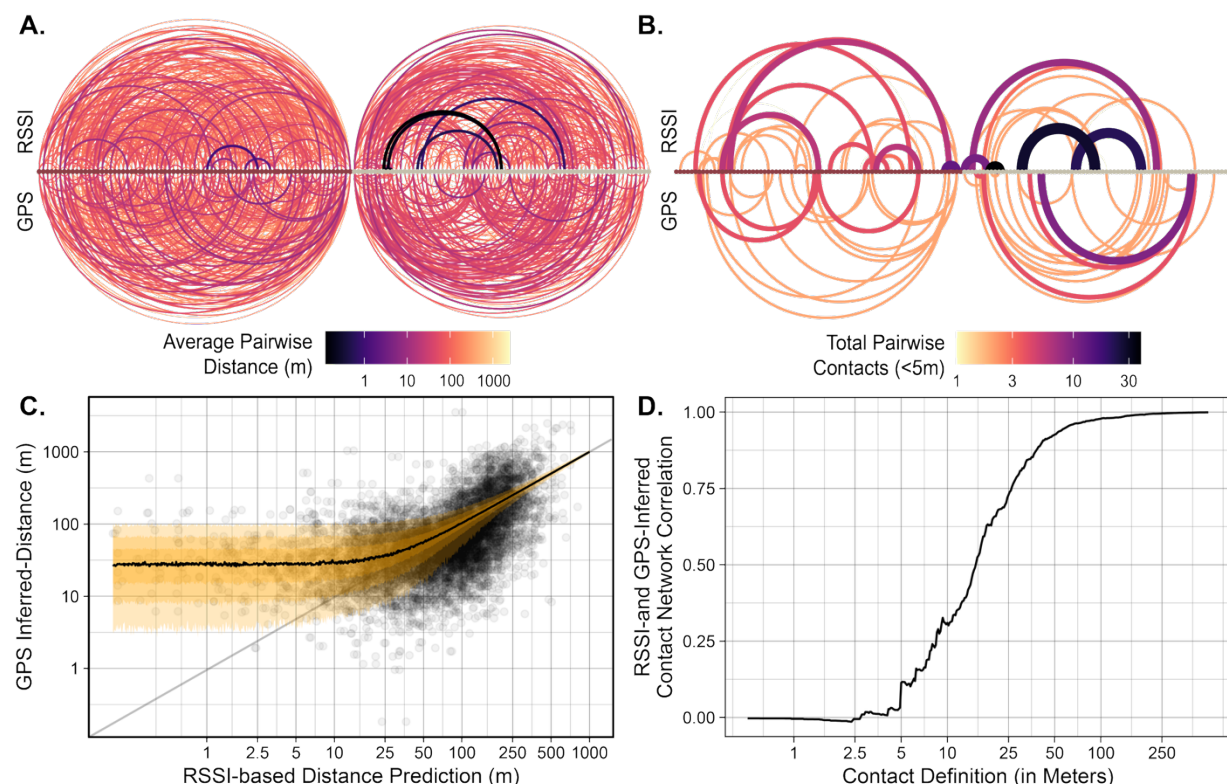
Figure 7: (A) GPS- and RSSI-inferred average pairwise distance (line color and weight) and (B) total contact (<5 m, line color and weight) networks describe different patterns of spatial interactions, particularly at closer pairwise distances. RSSI predictions are conditioned on tag random effects, tag-measured weather data. Nodes within networks are individual bats tagged in 2023 (left, red) or 2024 (right, grey). (C) The disparity in pairwise distance from RSSI predictions and GPS observations is most apparent at distances <50 m (points). Simulations using empirical GPS error recover the observed pattern of inflated pairwise distance estimates (median, 50%, 85%, and 95% intervals shown by black line and shaded orange regions). (D) Similarly, the correlation between RSSI and GPS total contact network declines for contact definitions <50 m, and contact networks are largely uncorrelated for contacts <5 m.

References

576

577 Akaike, H. 1998. Information theory and an extension of the maximum likelihood principle.

578 Pages 199-213 Selected papers of hirotugu akaike. Springer.

579 Barton, K. 2009. MuMIn: multi-model inference. http://r-forge. r-project. org/projects/mumin/.

580 Bettaney, E. M., R. James, J. J. H. St Clair, and C. Rutz. 2015. Processing and visualising

581 association data from animal-borne proximity loggers. Animal Biotelemetry **3**:27.

582 Böhm, M., M. R. Hutchings, and P. C. L. White. 2009. Contact Networks in a Wildlife-

583 Livestock Host Community: Identifying High-Risk Individuals in the Transmission of

584 Bovine TB among Badgers and Cattle. PLoS One **4**:e5016.

585 Boyland, N. K., R. James, D. T. Mlynski, J. R. Madden, and D. P. Croft. 2013. Spatial proximity

586 loggers for recording animal social networks: consequences of inter-logger variation in

587 performance. Behavioral Ecology and Sociobiology **67**:1877-1890.

588 Brooks, M. E., K. Kristensen, K. J. Van Benthem, A. Magnusson, C. W. Berg, A. Nielsen, H. J.

589 Skaug, M. Machler, and B. M. Bolker. 2017. glmmTMB balances speed and flexibility

590 among packages for zero-inflated generalized linear mixed modeling. The R journal

591 **9**:378-400.

592 Craft, M. E. 2015. Infectious disease transmission and contact networks in wildlife and livestock.

593 Philos Trans R Soc Lond B Biol Sci **370**.

594 Cross, P. C., T. G. Creech, M. R. Ebinger, D. M. Heisey, K. M. Irvine, and S. Creel. 2012.

595 Wildlife contact analysis: emerging methods, questions, and challenges. Pages 1437-1447

596 Behavioral Ecology and Sociobiology. Springer.

597   Drewe, J. A., N. Weber, S. P. Carter, S. Bearhop, X. A. Harrison, S. R. Dall, R. A. McDonald,

598   and R. J. Delahay. 2012. Performance of proximity loggers in recording intra- and inter-

599   species interactions: a laboratory and field-based validation study. PLoS One **7**:e39068.

600   Frair, J. L., J. Fieberg, M. Hebblewhite, F. Cagnacci, N. J. DeCesare, and L. Pedrotti. 2010.

601   Resolving issues of imprecise and habitat-biased locations in ecological analyses using

602   GPS telemetry data. Philosophical Transactions of the Royal Society B: Biological

603   Sciences **365**:2187-2200.

604   Hartig, F. 2018. DHARMa: residual diagnostics for hierarchical (multi-level/mixed) regression

605   models. R Packag version 020.

606   He, P., J. A. Klarevas-Irby, D. Papageorgiou, C. Christensen, E. D. Strauss, and D. R. Farine.

607   2023. A guide to sampling design for GPS-based studies of animal societies. Methods in

608   Ecology and Evolution **14**:1887-1905.

609   Kays, R., S. Tilak, M. Crofoot, T. Fountain, D. Obando, A. Ortega, F. Kuemmeth, J. Mandel, G.

610   Swenson, T. Lambert, B. Hirsch, and M. Wikelski. 2011. Tracking Animal Location and

611   Activity with an Automated Radio Telemetry System in a Tropical Rainforest. The

612   Computer Journal **54**:1931-1948.

613   Kays, R., and M. Wikelski. 2023. The Internet of Animals: what it is, what it could be. Trends in

614   ecology & evolution.

615   Kluge, T., C. Groba, and T. Springer. 2020. Trilateration, Fingerprinting, and Centroid: Taking

616   Indoor Positioning with Bluetooth LE to the Wild. Pages 264-272 *in* 2020 IEEE 21st

617   International Symposium on "A World of Wireless, Mobile and Multimedia Networks"

618   (WoWMoM).

Krause, J., S. Krause, R. Arlinghaus, I. Psorakis, S. Roberts, and C. Rutz. 2013. Reality mining of animal social systems. Trends in Ecology and Evolution **28**:541-551.

Manlove, K., M. Wilber, L. White, G. Bastille-Rousseau, A. Yang, M. L. J. Gilbertson, M. E. Craft, P. C. Cross, G. Wittemyer, and K. M. Pepin. 2022. Defining an epidemiological landscape that connects movement ecology to pathogen transmission and pace-of-life. Ecol Lett.

Marfievici, R., A. L. Murphy, G. P. Picco, F. Ossi, and F. Cagnacci. 2013. How Environmental Factors Impact Outdoor Wireless Sensor Networks: A Case Study. Pages 565-573 *in* 2013 IEEE 10th International Conference on Mobile Ad-Hoc and Sensor Systems.

Merkle, J. A., M.-P. Poulin, M. R. Caldwell, M. P. Laforge, A. E. Scholle, T. L. Verzuh, and C. Geremia. 2024. Spatial–social familiarity complements the spatial–social interface: evidence from Yellowstone bison. Philosophical Transactions of the Royal Society B: Biological Sciences **379**:20220530.

Oksanen, J., F. G. Blanchet, R. Kindt, P. Legendre, P. R. Minchin, R. O'hara, G. L. Simpson, P. Solymos, M. H. H. Stevens, and H. Wagner. 2013. Package 'vegan'. Community ecology package, version **2**:1-295.

Paxton, K. L., K. M. Baker, Z. B. Crytser, R. M. P. Guinto, K. W. Brinck, H. S. Rogers, and E. H. Paxton. 2022. Optimizing trilateration estimates for tracking fine-scale movement of wildlife using automated radio telemetry networks. Ecology and evolution **12**:e8561.

Prange, S., T. Jordan, C. Hunter, and S. D. Gehrt. 2006. New Radiocollars for the Detection of Proximity among Individuals. Wildlife Society Bulletin **34**:1333-1344.

640   Ripperger, S., D. Josic, M. Hierold, A. Koelpin, R. Weigel, M. Hartmann, R. Page, and F.

641   Mayer. 2016. Automated proximity sensing in small vertebrates: design of miniaturized

642   sensor nodes and first field tests in bats. Ecology and evolution **6**:2179-2189.

643   Ripperger, S. P., G. G. Carter, R. A. Page, N. Duda, A. Koelpin, R. Weigel, M. Hartmann, T.

644   Nowak, J. Thielecke, M. Schadhauser, J. Robert, S. Herbst, K. Meyer-Wegener, P.

645   Wägemann, W. Schröder-Preikschat, B. Cassens, R. Kapitza, F. Dressler, and F. Mayer.

646   2020. Thinking small: Next-generation sensor networks close the size gap in vertebrate

647   biologging. PLOS Biology **18**:e3000655.

648   Rutz, C., M. B. Morrissey, Z. T. Burns, J. Burt, B. Otis, J. J. H. St Clair, and R. James. 2015.

649   Calibrating animal-borne proximity loggers. Methods in Ecology and Evolution **6**:656-

650   667.

651   Smith, J. E., and N. Pinter-Wollman. 2021. Observing the unwatchable: Integrating automated

652   sensing, naturalistic observations and animal social network analysis in the age of big

653   data. Journal of Animal Ecology **90**:62-75.

654   Snijders, L., D. T. Blumstein, C. R. Stanley, and D. W. Franks. 2017. Animal Social Network

655   Theory Can Help Wildlife Conservation. Trends in ecology & evolution **32**:567-577.

656   St Clair, J. J. H., Z. T. Burns, E. M. Bettaney, M. B. Morrissey, B. Otis, T. B. Ryder, R. C.

657   Fleischer, R. James, and C. Rutz. 2015. Experimental resource pulses influence social-

658   network dynamics and the potential for information flow in tool-using crows. Nature

659   Communications **6**:7197.

660   Suraci, J. P., J. A. Smith, S. Chamaillé-Jammes, K. M. Gaynor, M. Jones, B. Luttbeg, E. G.

661   Ritchie, M. J. Sheriff, and A. Sih. 2022. Beyond spatial overlap: harnessing new

662   technologies to resolve the complexities of predator–prey interactions. Oikos

663   **2022**:e09004.

664 Team, R. C. 2021. A language and environment for statistical computing.

665 Wilber, M. Q., A. Yang, R. Boughton, K. R. Manlove, R. S. Miller, K. M. Pepin, and G.

666   Wittemyer. 2022. A model for leveraging animal movement to understand spatio-

667   temporal disease dynamics. Ecol Lett **25**:1290-1304.

668 Wild, T. A., J. C. Koblitz, D. K. N. Dechmann, C. Dietz, M. Meboldt, and M. Wikelski. 2022a.

669   Micro-sized open-source and low-cost GPS loggers below 1 g minimise the impact on

670   animals while collecting thousands of fixes. PLoS One **17**:e0267730.

671 Wild, T. A., M. Wikelski, S. Tyndel, G. Alarcón-Nieto, B. C. Klump, L. M. Aplin, M. Meboldt,

672   and H. J. Williams. 2022b. Internet on animals: Wi-Fi-enabled devices provide a solution

673   for big data transmission in biologging. Methods in Ecology and Evolution.

674 Wild, T. A., G. Wilbs, D. K. N. Dechmann, J. E. Kohles, N. Linek, S. Mattingly, N. Richter, S.

675   Sfenthourakis, H. Nicolaou, E. Erotokritou, and M. Wikelski. 2024. Time

676   synchronisation for millisecond-precision on bio-loggers. Movement Ecology **12**:71.

677 Williams, H. J., L. A. Taylor, S. Benhamou, A. I. Bijleveld, T. A. Clay, S. de Grissac, U.

678   Demsar, H. M. English, N. Franconi, A. Gomez-Laich, R. C. Griffiths, W. P. Kay, J. M.

679   Morales, J. R. Potts, K. F. Rogerson, C. Rutz, A. Spelt, A. M. Trevail, R. P. Wilson, and

680   L. Borger. 2020. Optimizing the use of biologgers for movement ecology research.

681   Journal of Animal Ecology **89**:186-206.

682 Wood, S. N. 2010. Fast Stable Restricted Maximum Likelihood and Marginal Likelihood

683   Estimation of Semiparametric Generalized Linear Models. Journal of the Royal

684   Statistical Society Series B: Statistical Methodology **73**:3-36.

685   Yang, A., M. Q. Wilber, K. R. Manlove, R. S. Miller, R. Boughton, J. Beasley, J. Northrup, K.

686   C. VerCauteren, G. Wittemyer, and K. Pepin. 2023. Deriving spatially explicit direct and

687   indirect interaction networks from animal movement data. Ecology and evolution

688   **13**:e9774.

689   Yu, H., G. J. Amador, A. Cribellier, M. Klaassen, H. J. de Knegt, M. Naguib, R. Nijland, L.

690   Nowak, H. H. T. Prins, L. Snijders, C. Tyson, and F. T. Muijres. 2024. Edge computing

691   in wildlife behavior and ecology. Trends in ecology & evolution **39**:128-130.

692